remote sensing

MDPI

Article

Modeling Barrier Island Habitats Using Landscape Position Information

Nicholas M. Enwright [1,2,*], Lei Wang [2], Hongqing Wang [3], Michael J. Osland [1], Laura C. Feher [1], Sinéad M. Borchert [4] and Richard H. Day [1]

1 U.S. Geological Survey, Wetland and Aquatic Research Center, Lafayette, LA 70506, USA; mosland@usgs.gov (M.J.O.); lfeher@usgs.gov (L.C.F.); dayr@usgs.gov (R.H.D.)
2 Louisiana State University, Department of Geography and Anthropology, Baton Rouge, LA 70803, USA; leiwang@lsu.edu
3 U.S. Geological Survey, Wetland and Aquatic Research Center, Baton Rouge, LA 70803, USA; wangh@usgs.gov
4 Borchert Consulting at the U.S. Geological Survey, Wetland and Aquatic Research Center, Lafayette, LA 70506, USA; sinead_borchert@fws.gov
* Correspondence: enwrightn@usgs.gov; Tel.: +1-337-266-8613

Received: 25 March 2019; Accepted: 22 April 2019; Published: 24 April 2019

Abstract: Barrier islands are dynamic environments because of their position along the marine–estuarine interface. Geomorphology influences habitat distribution on barrier islands by regulating exposure to harsh abiotic conditions. Researchers have identified linkages between habitat and landscape position, such as elevation and distance from shore, yet these linkages have not been fully leveraged to develop predictive models. Our aim was to evaluate the performance of commonly used machine learning algorithms, including K-nearest neighbor, support vector machine, and random forest, for predicting barrier island habitats using landscape position for Dauphin Island, Alabama, USA. Landscape position predictors were extracted from topobathymetric data. Models were developed for three tidal zones: subtidal, intertidal, and supratidal/upland. We used a contemporary habitat map to identify landscape position linkages for habitats, such as beach, dune, woody vegetation, and marsh. Deterministic accuracy, fuzzy accuracy, and hindcasting were used for validation. The random forest algorithm performed best for intertidal and supratidal/upland habitats, while the K-nearest neighbor algorithm performed best for subtidal habitats. A posteriori application of expert rules based on theoretical understanding of barrier island habitats enhanced model results. For the contemporary model, deterministic overall accuracy was nearly 70%, and fuzzy overall accuracy was over 80%. For the hindcast model, deterministic overall accuracy was nearly 80%, and fuzzy overall accuracy was over 90%. We found machine learning algorithms were well-suited for predicting barrier island habitats using landscape position. Our model framework could be coupled with hydrodynamic geomorphologic models for forecasting habitats with accelerated sea-level rise, simulated storms, and restoration actions.

Keywords: habitat modeling; machine learning; geocomputation; dune; wetlands; marsh; lidar; uncertainty; restoration; monitoring

1. Introduction

Barrier islands are subaerial expressions consisting of wave-, wind-, and/or tide-deposited sediments [1]. These islands are found along portions of every continent, except Antarctica [2], and provide numerous important ecosystem services including storm surge reduction, wave attenuation, erosion control to the mainland, habitat for fish and wildlife, carbon sequestration in marshes,

water catchment and purification, recreation, and tourism [3–5]. Barrier islands tend to be dynamic because of their location along the estuarine–marine interface. Collectively, these factors make barrier island monitoring a critical need of natural resource managers for coastal management, such as planning for coastal protection and restoration. As a result, natural resource managers often use habitat maps developed by geographers and remote sensing scientists to gain insights into how these islands are changing over time [6–10]. Besides gradual changes caused by constant forces, such as currents and tides, barrier islands face numerous threats including hurricanes, accelerated sea-level rise, oil spills, and anthropogenic impacts [11]. These threats are likely to influence the future of barrier islands in the latter part of the 21st century, especially as climate-related threats to coastal areas are expected to increase in the future [12,13]. Thus, to better inform both current and future management decisions, resource managers often use scientific models that predict what barrier island systems may look like in the future with regard to morphology [14,15] and habitat for fish and wildlife [16].

Geomorphology is a critical component of barrier island habitat configuration, as certain foundation species [17] such as saltmeadow cordgrass (*Spartina patens* (Aiton) Muhl.), sea oats (*Uniola paniculata* L.), and slash pine (*Pinus elliottii*) tend to thrive in specific topographic settings or disturbance regimes [18]. Geomorphology regulates many abiotic factors that influence the performance of foundation plant species, including wave energy, salinity, inundation frequency, sea spray, Aeolian transport, and nutrient availability [19]. Researchers have established linkages between barrier island habitats and specific landscape position variables, such as distance from shoreline [19] and elevation [16,19–21].

Geocomputational models can incorporate landscape position information, including elevation and relative topography, to predict barrier island geomorphic features and habitats. For example, Halls et al. [21] developed a rule-based model that used landscape position to produce maps of geomorphic features (e.g., intertidal, supratidal, dune, hummock, swale, and overwash) using information extracted from a digital elevation model (DEM) for an area in North Carolina, USA. To predict geomorphic features, their model used elevation relative to tidal datums, relative topography, shape, and general location information (e.g., proximity). Similarly, Gutierrez et al. [14] developed a Bayesian network to model barrier island morphologic characteristics, including dune crest height, beach presence–absence, and beach width, using contemporary data such as a lidar-based DEM and orthophotography for Assateague Island, off the coasts of Maryland and Virginia, USA. Their approach also used data representing longer-term, larger-scale processes, including long-term shoreline change rates, barrier island width, barrier island elevation, proximity to inlets, and anthropogenic modification. Researchers often use data-driven, machine learning algorithms such as K-nearest neighbor (KNN) [22,23], support vector machine (SVM) [24,25], and random forest (RF) [26,27] to develop geocomputational models to make predictions from geospatial data. These algorithms could be effective tools for determining the relationship between landscape position and barrier island habitats. For example, Foster et al. [16] developed a naïve Bayes model to predict the overall habitat coverage based on elevation for Cape Canaveral Florida, USA, under alternative sea-level rise scenarios. Despite these productive examples and the demonstrated importance of landscape position, most researchers have not fully leveraged landscape position–habitat linkages to develop predictive models.

Incorporation of elevation uncertainty for extracting elevation-dependent habitats and post-processing model results using expert knowledge of barrier island habitats may enhance machine learning-based habitat prediction for barrier islands. Habitats on barrier islands can be tied to tidal regimes [28], which could allow for specific models to be developed for each tidal regime. Researchers can extract these tidal regimes directly from DEMs by using information regarding locally relevant tidal datums, such as extreme high water spring (EHWS), extreme low water spring (ELWS), and storm water levels [21,28,29]. When using automated extraction of elevation-dependent habitats, researchers are advised to address vertical uncertainty in DEMs [30–32]. This is critical for low-relief environments, such as barrier islands, where centimeters can make a difference in the exposure to physically demanding abiotic conditions (e.g., inundation, salt spray, wave energy) [19,20]. Enwright et al. [32] highlighted the impact of the treatment of vertical uncertainty within intertidal areas. Relative topography can be

helpful for extracting dune habitats [21,28,33], yet elevation relative to storm water levels can also be a factor, as dunes can be eroded by high wave runup during storms [5]. Thus, elevation uncertainty analyses could also be used to evaluate the likelihood of areas depicted by a DEM being above a common extreme storm water level [28]. Data-driven, machine learning algorithms are powerful tools for identifying patterns and relationships in data; however, one potential issue is that they require the assumption that the data used to train the model is representative of the phenomena being modeled. Because change can sometimes occur rapidly on a barrier island, post-processing could be used to ensure that spatially explicit habitat predictions match our expectations based on expert theoretical knowledge of the specific barrier island being modeled (e.g., for a high-energy barrier island we would not expect marsh to be located on the ocean-facing shoreline [34]).

Here, we build upon recent barrier island habitat model efforts by Foster et al. [16], Halls et al. [21], and Young et al. [19] to develop a habitat model for Dauphin Island, Alabama, USA. Our model incorporates elevation uncertainty for elevation-dependent habitat extraction and yields spatially explicit predictions of general barrier island habitats based on landscape position information such as elevation, distance from shoreline, and relative topography (Figure 1). For our study, we explored three research questions: (1) how well can machine learning algorithms, such as KNN, SVM, and RF, predict contemporary barrier island habitats from landscape position information; (2) does the use of post-processing routines, such as expert rules based on the theoretical understanding of a barrier island (e.g., marsh should not be located along the high-energy shoreline of the island), enhance model accuracy; and (3) how well does this model generalize to predict historical habitats (i.e., hindcast)?

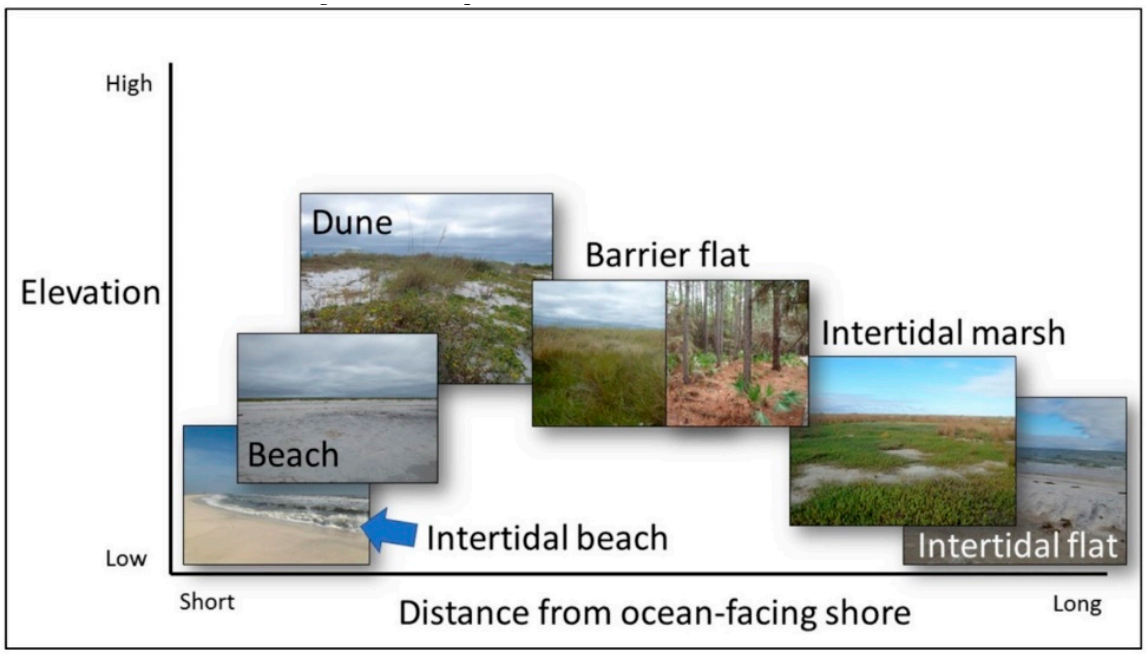

Figure 1. Hypothesized relationship between elevation and distance from ocean-facing shoreline for general barrier island habitats based on literature [19,35].

2. Materials and Methods

2.1. Study Site

Dauphin Island is part of a 105 km-wide Mississippi–Alabama, wave-dominated barrier island chain (Figure 2) [36,37]. The island is backed by the shallow (<4 m deep) Mississippi Sound [37] and is flanked to the east by Mobile Bay. In 2015, the length of Dauphin Island was about 25 km, and the subaerial portion of the island was estimated to be about 15.8 km^2 [28]. Situated in the northern Gulf of Mexico, Dauphin Island experiences diurnal tides with a mean tidal range of about 0.36 m (i.e., mean

low water to mean high water), based on observations during the most recent North American Tidal Datum Epoch (NTDE; 1983 to 2001) from a National Oceanic and Atmospheric Administration tide gauge (station ID: 8735180) on the island. We developed the modeling domain for this study (dashed outline in Figure 2) by buffering the maximum extent of Dauphin Island shorelines from 1940 to 2015 [38] by 2.5 km. We used Esri ArcMap 10.5.1 (Redlands, California, USA) for all spatial analyses.

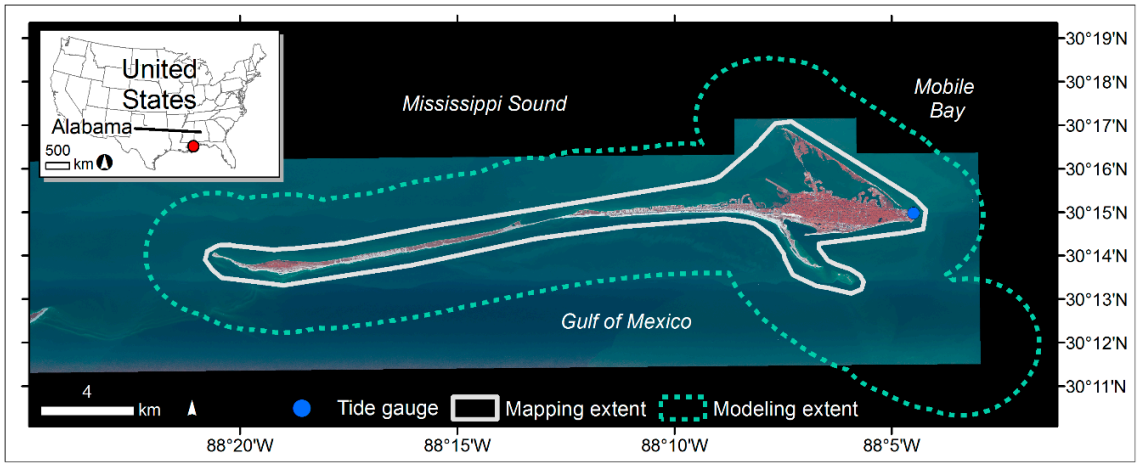

Figure 2. Modeling domain and the extent of baseline mapping data for habitat modeling effort on Dauphin Island, Alabama, USA. The basemap source data is 0.3 m color-infrared orthophotography acquired in December 2015 by Digital Aerial Solutions, LLC (Riverview, Florida, USA) and the U.S. Geological Survey (USGS). The area that is outside the 2015 imagery acquisition zone is shown in black.

2.2. Barrier Island Habitat

We set our model targets to be generalized habitat classes from a geomorphology-based habitat classification scheme that was recently used for a 2015 Dauphin Island habitat map [28] (Figure 3; Table A1). The habitat generalizations we applied involved combining habitat classes that may occupy the same geomorphic setting, yet are regulated by factors we did not include in our model, such as disturbance. Specifically, these included combining meadow and unvegetated barrier flat habitats into a single habitat class (i.e., barrier flat) and, likewise, combining forest and scrub/shrub into a single habitat class (i.e., woody vegetation). Each habitat in the model classification scheme was linked to a tidal zone (i.e., subtidal, intertidal, supratidal/upland; Figure 3). Our research questions were largely focused on predicting habitats; therefore, we did not make any predictions of changes to developed areas. These developed areas were extracted from the 2015 Dauphin Island habitat map and excluded from the machine learning model input and output.

Figure 3. Examples of the habitat classes for the barrier island habitat modeling effort on Dauphin Island, Alabama, USA. The classes are linked to tidal regime (see legend in lower left corner of the figure). The developed class was not shown since it was not explicitly modeled in this effort. Adapted from Enwright et al. [28] with permission.

2.3. Remote Sensing Data and In Situ Data

We used topobathymetric DEMs (TBDEMs) as the primary data source for landscape position information. The contemporary TBDEM was developed from a 1 m bare-earth DEM from lidar data collected in January 2015 by Digital Aerial Solutions, LLC (DAS, Riverview, Florida, USA). The TBDEM was produced by DAS and the U.S. Geological Survey (USGS). The contemporary bathymetric data for much of the nearshore area were from a 20 m DEM developed from single-beam sonar surveys by the USGS in 2015 [39]. Bathymetric data for the remainder of the study area were from the 3 m USGS Coastal National Elevation Database (CoNED) TBDEM [40] for the northern Gulf of Mexico, which included historical data from various periods between 1920 through 1988. We developed a seamless 10 m TBDEM by converting the rasters to points and using inverse distance-weighted interpolation to combine the datasets. The rationale for selecting 10 m for the model resolution was to use a spatial resolution that could be compatible with irregular grids from hydrodynamic numerical models that are commonly used for forecasting geomorphology [15].

The CoNED TBDEM was used for the hindcast TBDEM. Topographic data for the subaerial portion for most of the island in this dataset were from data collected via the USGS Experimental Advanced Airborne Research Lidar [41] in 2007, although a small area along the northern portion of eastern Dauphin Island and Little Dauphin Island (i.e., the narrow island on the northeastern end of the study area that runs from northwest to the southeast, Figure 2) was from lidar data from 2002 collected by Mobile County, Alabama. We resampled the CoNED to 10 m using bilinear interpolation.

We used orthophotography as ancillary data for model validation via photointerpretation. The contemporary orthophotography was ~0.3 m color-infrared aerial orthophotography acquired on 4 December 2015, by DAS and the USGS. The imagery was collected with a Leica ADS100 digital camera (Wetzlar, Germany) when water levels were near or just below mean sea level (MSL). The hindcast orthophotography was 0.5 m true color orthophotography collected with a Leica ADS40 digital camera (Wetzlar, Germany) by the USGS on 1 February 2008 for all but the western tip of Dauphin island. For this area, we used 1 m orthophotography captured with a Z/I digital mapping camera by

Photo Science, Inc. (Norcross, Virginia, USA) in October 2008 because of the lack of coverage in the February orthophotography.

We used tide data to identify the relationship between the North American Vertical Datum of 1988 (NAVD88), MSL, extreme spring tide levels, and extreme water levels. These data were obtained from the NOAA tide gauge on the eastern end of Dauphin Island (Figure 2). All TBDEMs were transformed from NAVD88 to MSL using relative height differences from the NOAA tide gauge during the current NTDE. Habitat type and elevation data were collected during two and a half weeks in November and December of 2015 at 67 different transects located across seven different sites on the eastern half of Dauphin Island [42]. These data were collected using a high-precision real-time kinematic (RTK) global positioning system (GPS) connected to a Global Navigation Satellite System (GNSS; Trimble R10 and TSC3, Trimble, Sunnyvale, California, USA). We used these data to develop two separate relative error assessments for the 2015 DEM [28,32]. The first assessment explored relative error for intertidal and low-lying herbaceous areas [32], whereas the second assessment quantified relative error in dunes [28]. We assumed that the error and bias in the historical TBDEM were similar to the contemporary TBDEM.

2.4. Probability Surfaces

We used Monte Carlo simulations to develop probability surfaces that indicated the likelihood that a pixel in the TBDEM was either in an intertidal geomorphic setting or above an extreme storm water level. To do this, we simulated the propagation of error uncertainty using information from the relative error assessments (i.e., error and bias). For subaerial areas, the Monte Carlo simulation to create the probability surface related to intertidal areas used the assessment from intertidal and low-lying herbaceous areas, whereas the Monte Carlo simulation for the likelihood of being above a storm water level used the dune assessment. For submerged areas for both simulations, we used recommendations from Byrnes et al. [43] for the root mean square error of bathymetry data for nearshore waters, and we assumed bias was negligible. The lower and upper elevation thresholds for the intertidal probability surface were the lowest astronomical tide and the highest astronomical tide observed during the NTDE at Dauphin Island, respectively [44]. The elevation threshold for the extreme water probability surface was set to be the extreme water level with a 10% annual exceedance probability from the NOAA's Extreme Water Analyses for Dauphin Island [45], which was updated for 2016 (1.13 m relative to MSL) to account for the sea-level rise trend observed at the Dauphin Island tide gauge [46]. For more information on the probability rasters and Monte Carlo simulations, see Enwright et al. [28,32].

2.5. Tidal Zone Determination

Because the habitat classes were linked to tidal zones (Figure 3), it was important to be able to automate the extraction of tidal zones from the TBDEM. We used the intertidal probability surfaces to separate the model domain by tidal zone. Subtidal areas were pixels with a probability of being intertidal that were less than 0.5 and had an elevation less than MSL. Intertidal areas were areas with a probability of being intertidal greater than or equal to 0.5. We used the connectivity of the raster cells as defined by the queen's move rule, which searches for interconnected cells in both cardinal and diagonal directions, to remove isolated low-lying areas from the intertidal zone [47]. After subtidal and intertidal areas were identified, the remaining areas, which included the isolated low-lying areas, were classified as supratidal/upland.

2.6. Predictor Variable Processing

We used the TBDEM to develop numerous landscape position predictor variables based on literature-derived linkages of landscape position to barrier island ecology and habitat distribution [16,19–21]. The predictor variables were related to elevation or X, Y coordinates (i.e., proximity and direction; Figure 4). We determined the value of these predictor variables for each 10 m pixel in the TBDEM. We used the topographic position index [48] as a measure of relative topography. This was calculated by subtracting the elevation for a single pixel to that of a neighborhood.

Halls et al. [21] used the topographic position index to extract dune habitat. The elevation to the south variables were calculated by taking the median of the maximum elevation for three 22-degree wedge-shaped kernels radiating to the south with radii of 1 km and 8 km. The distance from the Mobile-Tensaw River Delta was a cost distance, which restricted the distance calculation to subtidal areas identified from the TBDEMs. To do this, we created a cost surface that only included subtidal areas (i.e., intertidal, supratidal, and upland areas were set to "NoData"). For the Euclidean direction from the center variable (Figure 4), we determined Euclidean direction from centroids of 5 m cross-shore transects. We recoded this variable to 1 for directions between 90 degrees and 270 degrees, otherwise the value was set to 0.

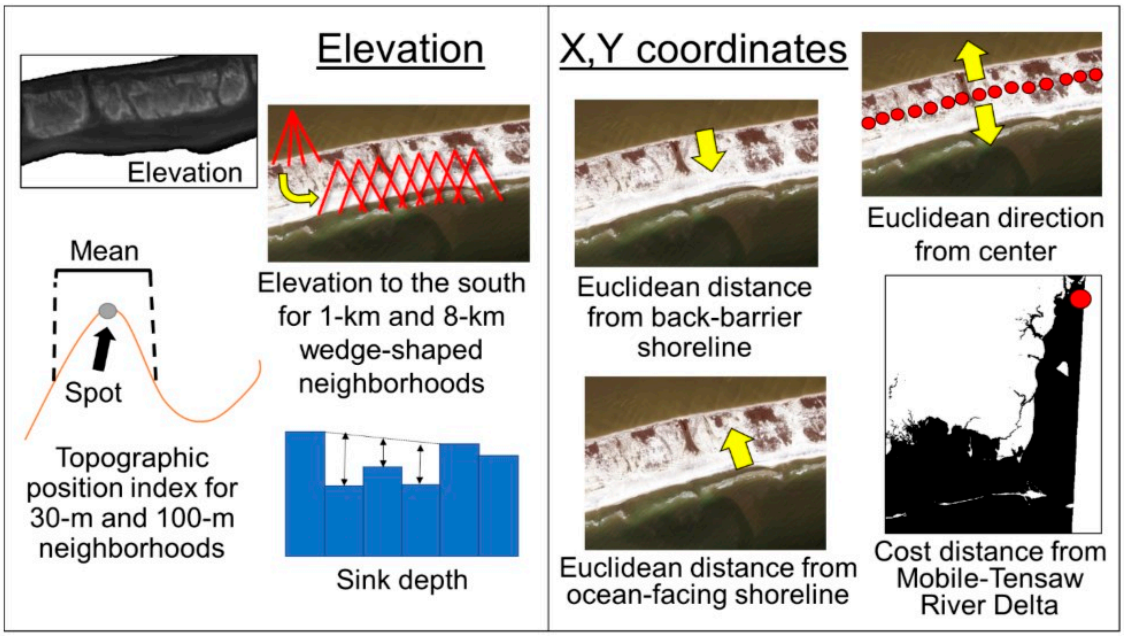

Figure 4. Landscape position predictor variables for the barrier island habitat modeling effort on Dauphin Island, Alabama, USA. The imagery source data is 0.3 m color-infrared orthophotography acquired in December 2015, and the elevation data source data is a 1 m digital elevation model from January 2015. Both of these data were collected by Digital Aerial Solutions, LLC (Riverview, Florida, USA) and the U.S. Geological Survey.

2.7. Habitat Modeling

The first step in the modeling process was to develop a habitat model for each tidal zone from contemporary data (Figure 5). We used the 2015 habitat map [28] (solid outline in Figure 2) to develop training and validation datasets. These data were stratified among tidal zones and by habitat types within tidal zones to be proportional to the habitat strata from the 2015 habitat map [28]. With a minimum of 42 training points, we ensured that we had at least 30 training points for each class for training datasets made from 70% random permutations. To limit spatial autocorrelation issues with training data, we created random points per class through an iterative process aimed at maximizing the minimum distance between points. We used a similar approach to control the minimum sample distance per habitat class for all random samples developed in this effort (i.e., training and validation data for the contemporary and hindcast outputs). While our approach included model assessment, via data division of training data through both cross-validation and permutation, we also developed a separate validation dataset. This dataset included 1000 points per tidal zone stratified by the areal coverage of habitat classes predicted per tidal zone, and data did not include any data division. Areas within 10 m of the training samples were excluded from the validation set. Furthermore, to avoid the influence from anthropogenic development, we buffered developed areas from the 2015 habitat map by 10 m and excluded these areas from the validation sampling frame. Mapping intertidal areas

from aerial orthophotography can be difficult since the imagery just shows water levels from a single snapshot. Thus, we excluded intertidal areas that were below MSL in the contemporary TBDEM from the contemporary validation assessment. Following guidelines from Congalton and Green [49] for accuracy assessment, we attempted to include at least 50 points per class, but we were only able to include around 30 points in woody wetland and water-fresh habitats because of the limited areal coverage of these habitats and the constraint of the minimum distance criterion.

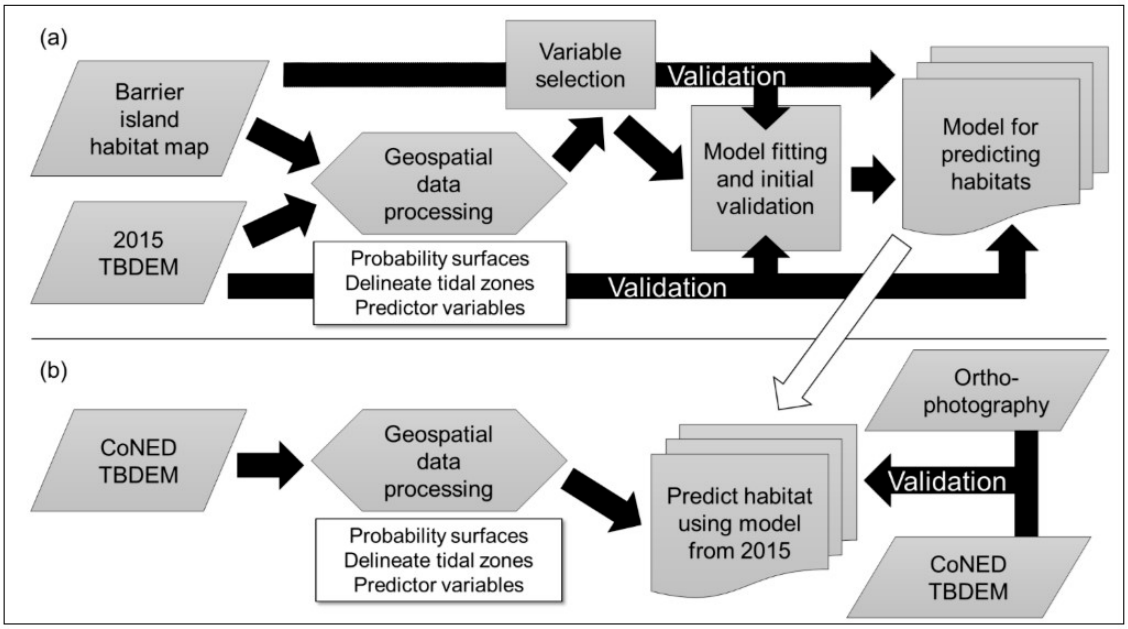

Figure 5. Workflow for the barrier island habitat model development for Dauphin Island, Alabama, USA. (**a**) Overview of process for developing and validating the contemporary model for predicting barrier island habitats using a habitat map and a topobathymetric (TBDEM) from 2015; (**b**) Overview of the process for predicting barrier island habitats using historical data from the USGS Coastal National Elevation Dataset (CoNED) TBDEM using the model fitted with contemporary data (i.e., hindcast).

We used MathWorks® MATLAB 2016b (Natick, Massachusetts, USA) for model fitting and prediction. We used the MATLAB Classification Learner application in the Statistics and Machine Learning Toolbox to fit and assess KNN, SVM, and RF models for several MATLAB model presets, such as various neighborhood sizes, weights, and distance metrics for KNN models, and kernel scale and kernel function for SVM models (Tables A2–A4). We opted to use standard MATLAB model presets to avoid overfitting our model since our model was developed from a single snapshot of barrier island habitat data, and barrier islands are dynamic ecosystems that can change gradually from coastal processes including currents and tides or rapidly from episodic events such as storms. Based on five permutations of the training data, we selected the best performing KNN and SVM models using five-fold cross-validation for each tidal zone (Tables A2–A4; Figure A1). These models were combined with the RF models for further validation. For KNN and SVM models, we followed general recommendations to standardize the predictor variables to scale the feature space distance for these models [50]. Table 1 lists the variables used per model with rationale. As previously mentioned, the selection of these specific predictor variables was based on literature and our theoretical understanding of barrier island habitats. Figure A2 shows the unbiased relative importance from a random forest ensemble model with 100 learners. To illustrate how landscape position can influence barrier island habitats, we used the MATLAB Distribution Fitting application in the Statistics and Machine Learning Toolbox to plot univariate probability density functions for elevation and distance from the ocean-facing shoreline for the supratidal/upland habitats. For the probability density plots, we used non-parametric curves with bandwidths that best fit the data based on visual inspection.

Table 1. Response variables (i.e., habitat classes) and predictor variables per tidal zone for the habitat model for Dauphin Island, Alabama, USA.

Tidal Zone	Habitat (Number of Training Points)	Predictor Variables and Source	Source
Subtidal	Water-estuarine (1000) Water-marine (1000)	(1) Distance from Mobile-Tensaw River Delta (2) Direction from center	(1–2) [44]
Intertidal	Intertidal flat (252) Intertidal beach (50) Intertidal marsh (121)	(1) Elevation (2) Elevation to the south (8 km) (3) Distance from ocean-facing shoreline (4) Distance from back-barrier shoreline	(1) [16,19,20,44] (2) [18] (3–4) [19]
Supratidal/ upland	Barrier flat (484) Beach (99) Dune (184) Water-fresh (43) Woody vegetation (327) Woody wetland (43)	(1) Elevation (2) Elevation to the south (1 km) (3) Topographic position index (30 m) (4) Topographic position index (100 m) (5) Distance from ocean-facing shoreline (6) Distance from back-barrier shoreline	(1) [16,19,20,44] (2) [18] (3–4) [21,28,33] (5–6) [19]

To avoid overfitting a single model, we trained 100 models per tidal zone from 70% of the training set selected by random permutations. For each cell, the majority habitat class of the 100 predictions was chosen as the final prediction. The intertidal zone and the supratidal/upland zone models were applied to each cell in the 10 m raster; however, to increase efficiency of the subtidal zone models, we made predictions for a 100 m raster and then converted these data to a 10 m raster using inverse distance-weighted interpolation.

We used the validation points to assess the overall, the producer's, and the user's accuracies for each class. For each assessment, we calculated a deterministic and fuzzy estimate for all accuracy statistics following guidelines by Congalton and Green [49] and Woodcock and Gopal [51]. The fuzzy accuracy estimate allows classification of: (1) exact match (e.g., woody vegetation in model results and orthophotography); (2) acceptable match related to landscape position and geomorphic setting (e.g., calling a location intertidal beach or water-marine along ocean-facing shoreline); and (3) unacceptable/error (e.g., intertidal marsh located on the high-energy, ocean-facing shoreline). Fuzzy accuracy is well-suited for assessing barrier island habitats because of dynamic transitions like open water classes and intertidal classes, which are dependent on water level.

To determine the best model per tidal zone (i.e., from the subset of models, which included the RF models and the top-performing KNN and SVM models), we used the tidal zone delineations from the contemporary 10 m TBDEM to extract the validation points that fell within the tidal zone. However, because the validation data were from the 1 m 2015 habitat map, there may have been some discrepancies between the reference labels within a tidal zone because of temporal lag and spatial resolution differences. Thus, we omitted validation points that had a reference label other than what would be expected in the tidal zone being assessed (e.g., we omitted points that had a reference label of intertidal beach from the supratidal/upland zone). Similar to Foody [52], we used McNemar's test to assess whether there was a significant difference in model performance between the top-performing models per tidal zone (Table A5).

Next, we combined the best model per tidal zone and tested whether the application of a suite of post-processing routines enhanced model results. These included the application of a majority filter to reduce noise along with several user-defined constraints based on the theoretical understanding of barrier island habitats from the literature regarding elevation and X, Y coordinates [19,35,44]. For example, on non-fetch-limited barrier islands, emergent marsh vegetation typically occurs where wave energy is lower, whereas unvegetated intertidal mudflats or intertidal beach habitats are more common where wave energy is higher [34]. Therefore, intertidal marsh habitats found along the ocean-facing shore were changed to intertidal beach habitats. An additional example is that dunes are not expected to be sustainable at low-lying elevations, such as those below a common extreme

storm water level [5]. Therefore, dune habitats that had a probability less than 0.5 for being above the extreme storm water level were recoded to barrier flats [28]. These rules were applied in a step-wise fashion (Table A6). Some of the thresholds used were directly related to tidal datums (e.g., EHWS), whereas others, such as sink depth, were determined by trial-and-error with the final value being selected by visual inspection. We also explored whether the use of a four-pixel minimum mapping unit (MMU) impacted model performance. We selected four pixels as the maximum MMU based on visual inspection of results (i.e., small habitat areas can be lost if the MMU is too high). We used McNemar's test to assess whether there was a significant difference in model performance based on the level of model post-processing (Table A5).

Lastly, we applied the final model to hindcast habitats based on the predictor variables developed from the CoNED TBDEM (Figure 5). To validate the hindcast results, we developed a hindcast validation dataset with about 300 points per zone (n = 1029). These data consisted of stratified random points within each habitat model class. We assigned reference labels to the hindcast validation points through photointerpretation of the orthophotography and inspection of the TBDEM and probability surfaces, and we assessed deterministic and fuzzy map accuracies.

3. Results

Similar to Young et al. [19], we found that habitats on Dauphin Island were related to landscape position (Figure 6). For example, these plots showed that beach habitat tended to be located near the ocean-facing shore and had a mode for elevation of around 1 m relative to MSL, whereas woody vegetation had a mode for elevation of just under 2 m relative to MSL and was further away from the ocean-facing shoreline. Collectively, these plots confirmed that landscape position variables were important predictors for supratidal/upland habitats on Dauphin Island.

The top-performing models for the subtidal zone using five-fold cross validation were coarse KNN, fine gaussian SVM, and RF (Table A2). For the intertidal zone, the top performing models using five-fold cross validation were weighted KNN, cubic SVM, and RF (Table A3). Lastly, the top performing models for the supratidal/upland zone using five-fold cross validation were weighted KNN, quadratic SVM, and RF (Table A4). With more robust model development (i.e., using 100 random permutations of the training data) and assessment using the validation data from the 2015 habitat map, the performances of all of the models were similar for the subtidal zone (Figure A1); however, the coarse KNN model was selected for the subtidal zone based on visual inspection of the results. We did not run McNemar's test for the subtidal zone because each model had the same performance for the validation dataset. We found that RF performed the best for the intertidal and supratidal/upland zones (Figure A1). For the intertidal zone, we found that the RF model had a higher accuracy compared to either the KNN or SVM model (deterministic accuracy: $p < 0.001$; fuzzy accuracy: $p < 0.001$; Table A5). For the supratidal/upland zone, we found that the RF model had a higher accuracy compared to the KNN model (deterministic accuracy: $p < 0.05$; fuzzy accuracy: $p < 0.001$), but the results were not significantly different from the SVM model (deterministic accuracy: $p = 0.617$; fuzzy accuracy: $p = 0.126$; Table A5).

As previously mentioned, these models were combined to create the contemporary model results. The combined contemporary model had a deterministic overall accuracy of 66.9% and a fuzzy overall accuracy of 80.3% (Figure 7a,b; Table A7). The application of post-processing yielded a slight enhancement to the deterministic and fuzzy overall accuracies (Figure 7c,d; Table 2). We selected the model with post-processing and a four-pixel MMU as the final model. This model had a deterministic overall accuracy of 67.5% and a fuzzy overall accuracy of 82.1% (Figure 7e,f; Table 2). However, we did not find that the application of the MMU led to a negative impact on the results (Figure 7c–f). We found that the results of various levels of post-processing were not significantly different for the deterministic accuracy results; however, the fuzzy accuracies of both the models with post-processing (i.e., with and without the minimum mapping unit) were higher than the model results that did not include post-processing ($p < 0.001$; Table A5).

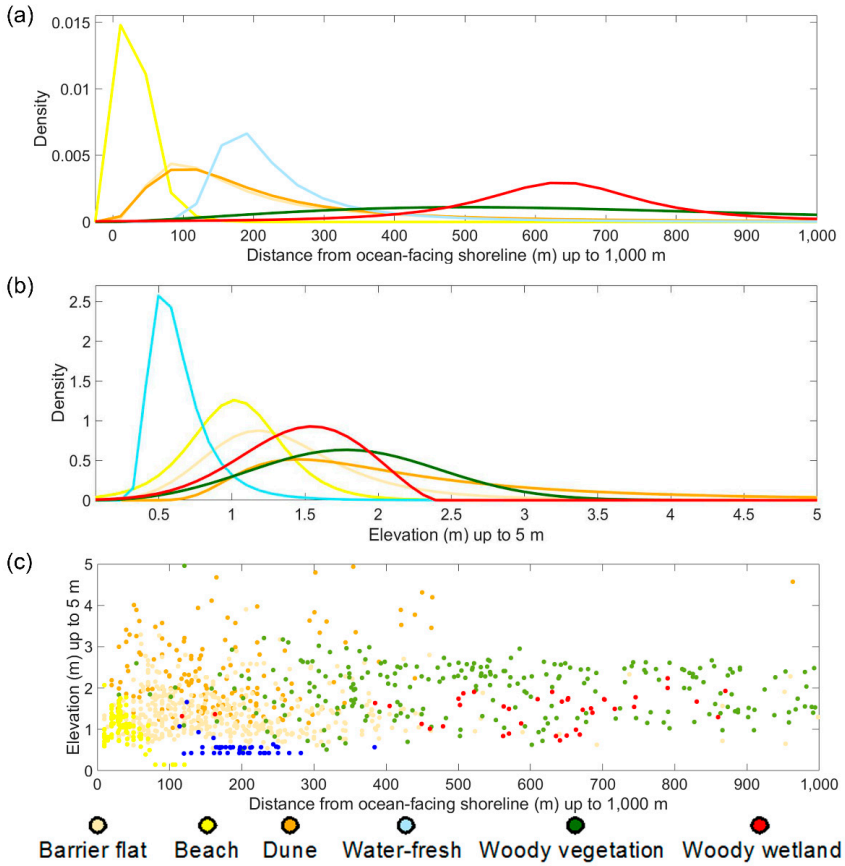

Figure 6. Probability density functions developed from the training data for the supratidal/upland zone from the contemporary (i.e., 2015) habitat model for Dauphin Island, Alabama, USA. (**a**) Distance (m) from the ocean-facing shoreline up to 1000 m; (**b**) Elevation (m) up to 5 m; and (**c**) a bivariate plot for these two variables.

While overall accuracy is a helpful measure, it is also important to assess class-specific performance reported by the producer's accuracy and user's accuracy. For the final contemporary model, the top three classes with regard to deterministic producer's accuracy were woody wetland (83.9%), water-fresh (82.1%), and woody vegetation (71.5%). The three classes with the highest fuzzy producer's accuracies were water-marine (97.1%), intertidal beach (94.6%), and woody wetland (83.9%). The classes with the lowest deterministic and fuzzy producer's accuracies were intertidal flat (60.0%) and dune (66.9%), respectively. The three classes with the highest deterministic user's accuracies were water-estuarine (98.3%), woody vegetation (86.7%), and water-marine (81.4%). The three classes with the highest fuzzy user's accuracies were water-estuarine (98.3%), woody vegetation (90.4%), and intertidal beach (85.8%). The classes with the lowest deterministic and fuzzy user's accuracies were intertidal beach (10.2%) and water-fresh (63.9%), respectively.

Figure 7a–f highlights the change in accuracy as a result from the use of fuzzy accuracy. For the final model, the use of fuzzy accuracy led to a median increase of producer's accuracy of 9.5% with an interquartile range of 15.2% (Figure 7e,f), while the user's accuracy was more variable with a median increase of user's accuracy of 3.9% with an interquartile range of 40.3%. In addition to the use of fuzzy accuracy, we found that the model results were often enhanced when post-processing routines were applied (Figure 7; Table A5). Compared to the original model results, the three highest magnitude changes in deterministic producer's accuracy as a result of the user-defined rules were water-fresh (−14.3%), intertidal beach (+10.8%), and dune (−5.7%). As a result of the user-defined rules, the three highest magnitude changes in deterministic user's accuracy were water-fresh (+11.0%), woody wetland (+6.9%), and dune (+6.4%). Figure 8 shows additional evidence to support the use of

post-processing by contrasting the western tip of Dauphin Island without post-processing (Figure 8a) and with post-processing (Figure 8b). Besides the reduction in dune habitat, a few notable differences included the reduction of intertidal beach areas that were found behind beach habitat, introduction of estuarine ponds within intertidal marsh, and the reduction in the salt-and-pepper effect. When comparing the areal coverage per supratidal/upland habitat, we saw the overall comparison of percent difference per habitat class more closely matched the 2015 habitat map [28]. Figure 9a shows the final contemporary model prediction map.

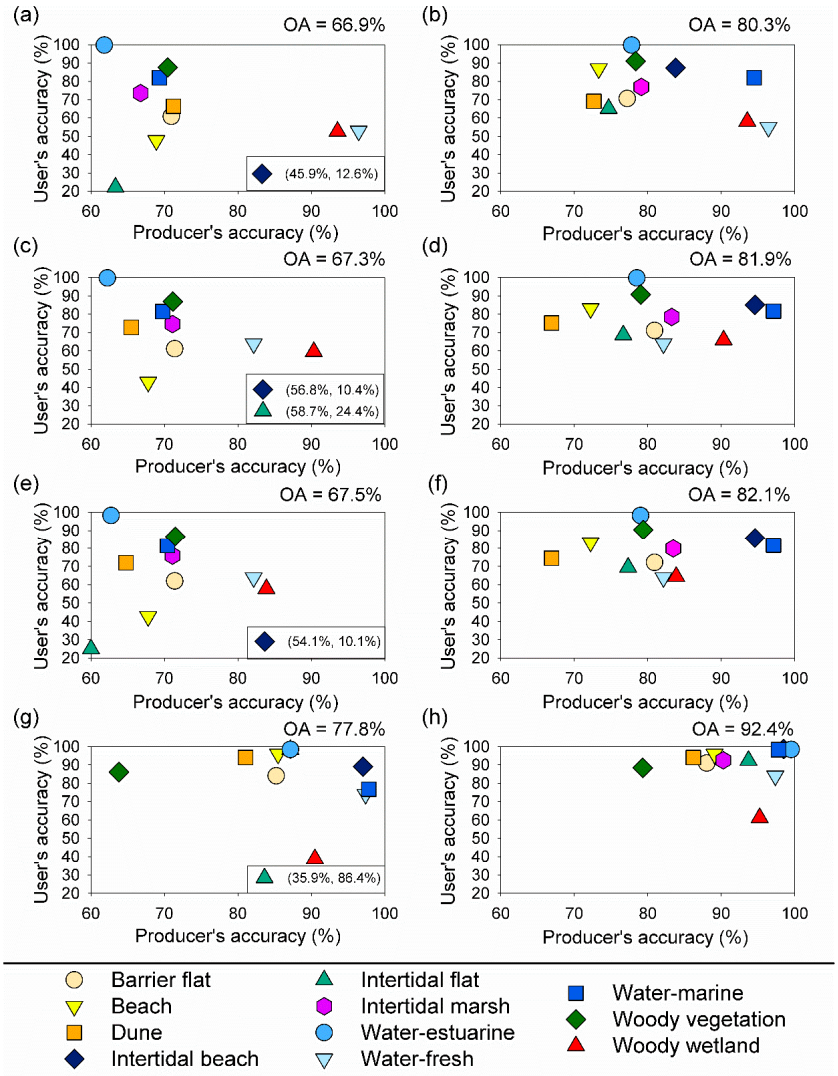

Figure 7. Producer's and user's accuracy results for the barrier island habitat model effort for Dauphin Island, Alabama, USA. (**a**) Class-specific deterministic accuracies for the final contemporary model without post-processing. (**b**) Class-specific fuzzy accuracies for the final contemporary model without post-processing. (**c**) Class-specific deterministic accuracies for the final contemporary model with post-processing, but no minimum mapping unit (MMU). (**d**) Class-specific fuzzy accuracies for the final contemporary model with post-processing, but no minimum mapping unit (MMU). (**e**) Class-specific deterministic accuracies for the final contemporary model with post-processing and a four-pixel MMU. (**f**) Class-specific fuzzy accuracies for the final contemporary model with post-processing and a four-pixel MMU. (**g**) Class-specific deterministic accuracies for the hindcast model with post-processing and a four-pixel MMU. (**h**) class-specific fuzzy accuracies for the hindcast model with post-processing and a four-pixel MMU. OA is the overall accuracy of the model results.

Table 2. Error matrix with deterministic and fuzzy accuracies for the final contemporary model results (i.e., with post-processing and a four-pixel minimum mapping unit) for Dauphin Island, Alabama, USA. For the off-diagonal cells, the first value indicates deterministic count, and the second value indicates the fuzzy count. BF: Barrier flat; B: Beach; CT: Column total; D: Dune; DPA: Deterministic producer's accuracy; DOA: Deterministic overall accuracy; DUA: Deterministic user's accuracy; FOA: Fuzzy overall accuracy; FPA: Fuzzy producer's accuracy; FUA: Fuzzy user's accuracy; IB: Intertidal beach; IF: Intertidal flat; IM: Intertidal marsh; RT: Row total; WE: Water-estuarine; WF: Water-fresh; WM: Water-marine; WV: Woody vegetation; and WW: Woody wetland.

	Class	Reference Data											DUA (%)	FUA (%)
		BF	B	D	IB	IF	IM	WE	WF	WM	WV	WW	RT		
Model data	BF	307	4;2	43;2	0;0	14;7	23;2	13;0	4;0	1;1	36;16	0;0	495	62.0	72.1
	B	9;9	61	1;1	1;15	1;4	4;0	1;0	0;0	7;28	0;1	0;0	143	42.7	83.2
	D	27;1	0;1	90	0;0	0;2	0;0	0;0	0;0	0;0	3;1	0;0	125	72.0	74.4
	IB	0;7	17;1	0;0	20	0;11	5;0	2;38	0;0	4;92	0;0	0;0	197	10.2	85.8
	IF	9;6	0;0	1;0	0;0	90	35;35	62;118	0;0	0;0	3;1	0;0	360	25.0	69.4
	IM	14;9	2;0	1;0	0;0	16;4	327	53;3	0;0	1;0	0;1	0;0	431	75.9	79.8
	WE	4;0	0;0	0;0	0;0	1;0	6;0	616	0;0	0;0	0;0	0;0	627	98.3	98.3
	WF	5;0	0;0	0;0	0;0	0;0	0;0	6;0	23	0;0	2;0	0;0	36	63.9	63.9
	WM	0;0	2;0	0;0	1;0	0;0	0;0	69;1	0;0	319	0;0	0;0	392	81.4	81.6
	WV	14;9	0;0	0;0	0;0	0;0	3;0	0;0	1;0	0;0	208	5;0	240	86.7	90.4
	WW	0;0	0;0	0;0	0;0	0;0	0;0	0;0	0;0	0;0	16;3	26	45	57.8	64.4
	CT	430	90	139	37	150	460	982	28	453	291	31	3091		
	DPA (%)	71.4	67.8	64.8	54.1	60.0	71.4	62.7	82.1	70.4	71.5	83.9			
	FPA (%)	80.9	72.2	66.9	94.6	77.3	83.5	79.0	82.1	97.1	79.4	83.9			
		DOA (%): 67.5; FOA (%): 82.1													

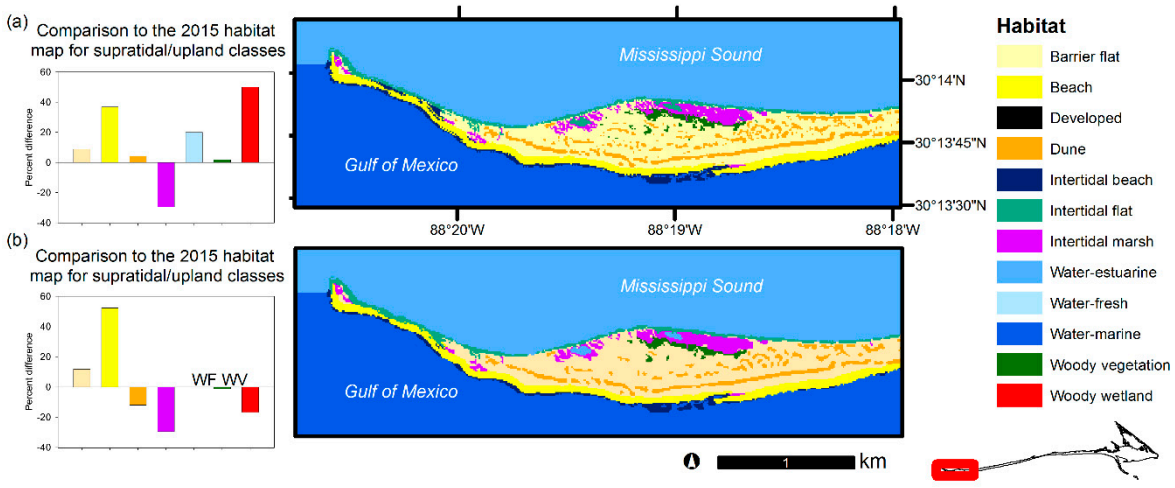

Figure 8. Barrier island habitat contemporary (i.e., 2015) habitat model outputs and percent difference comparison for supratidal/upland habitat compared to the 2015 habitat map Enwright et al. [28], Dauphin Island, Alabama, USA. (**a**) Contemporary model without post-processing. (**b**) Contemporary model with post-processing and four-pixel minimum mapping unit.

Overall, the model did generalize well for the hindcast with a deterministic overall accuracy of 77.8% and a fuzzy overall accuracy of 92.4% (Figure 7g,h; Figure 9b; Table 3). With regard to deterministic producer's accuracy, the top three classes were water-marine (97.8%), water-fresh (97.4%), and intertidal beach (97.0%). The three classes with the highest fuzzy producer's accuracies were water-estuarine (99.5%), intertidal beach (98.5%), and water-marine (97.8%). The classes with the lowest deterministic and fuzzy producer's accuracies were intertidal flat (35.9%) and woody vegetation (79.3%), respectively. The three classes with the highest deterministic user's accuracies were water-estuarine (98.4%), beach (95.9%), and dune (94.0%). The three classes with the highest fuzzy user's accuracies were water-estuarine (98.4%), water-marine (98.4%), and beach (95.9%). The classes with the lowest

deterministic and fuzzy user's accuracies were woody wetland/intertidal marsh (38.8%) and woody wetland (61.2%), respectively.

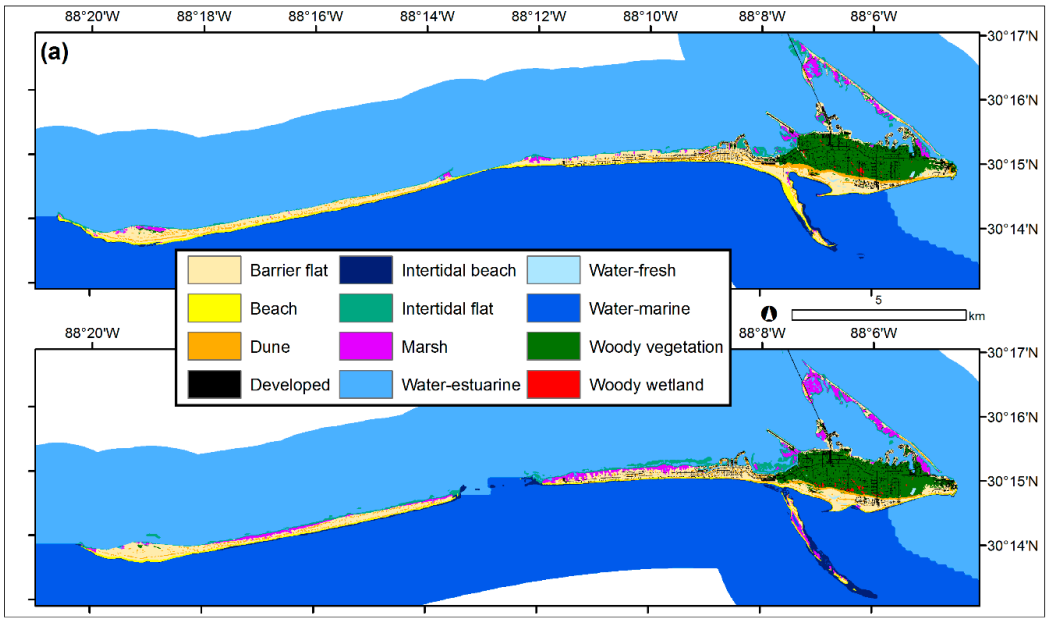

Figure 9. Final habitat model prediction maps for the barrier island for Dauphin Island, Alabama, USA. (**a**) Final contemporary model (i.e., 2015). (**b**) Final hindcast model (i.e., 2007 for most of the island and 2002 to for the northeast portion of the island).

Table 3. Error matrix with deterministic and fuzzy accuracies for the hindcast model results (i.e., with post-processing and a four-pixel minimum mapping unit) for Dauphin Island, Alabama, USA. For the off-diagonal cells, the first value indicates deterministic count and the second value indicates the fuzzy count. BF: Barrier flat; B: Beach; CT: Column total; D: Dune; DPA: Deterministic producer's accuracy; DOA: Deterministic overall accuracy; DUA: Deterministic user's accuracy; FOA: Fuzzy overall accuracy; FPA: Fuzzy producer's accuracy; FUA: Fuzzy user's accuracy; IB: Intertidal beach; IF: Intertidal flat; IM: Intertidal marsh; RT: Row total; WE: Water-estuarine; WF: Water-fresh; WM: Water-marine; WV: Woody vegetation; and WW: Woody wetland.

	Class	Reference Data											RT	DUA (%)	FUA (%)
		BF	B	D	IB	IF	IM	WE	WF	WM	WV	WW			
Model data	BF	121	5;2	5;3	0;0	0;0	0;0	1;0	1;0	0;0	1;5	0;0	144	84.0	91.0
	B	1;0	47	1;0	0;0	0;0	0;0	0;0	0;0	0;0	0;0	0;0	49	95.9	95.9
	D	2;0	0;0	47	0;0	0;0	0;0	0;0	0;0	0;0	1;0	0;0	50	94.0	94.0
	IB	0;0	0;0	0;0	65	1;7	0;0	0;0	0;0	0;0	0;0	0;0	73	89.0	98.6
	IF	0;0	0;0	0;0	0;1	57	5;3	0;0	0;0	0;0	0;0	0;0	66	86.4	92.4
	IM	3;1	0;0	0;0	1;0	7;85	62	0;0	0;0	0;0	1;0	0;0	160	38.8	92.5
	WE	0;0	0;0	0;0	0;0	1;0	0;0	183	0;0	2;0	0;0	0;0	186	98.4	98.4
	WF	6;2	0;0	0;0	0;0	0;0	0;0	0;1	37	0;0	2;2	0;0	50	74.0	84.0
	WM	0;0	1;0	0;0	0;0	1;0	0;0	0;25	0;0	89	0;0	0;0	116	76.7	98.4
	WV	5;1	0;0	2;0	0;0	0;0	2;0	0;0	0;0	0;0	74	1;1	86	86.1	88.4
	WW	0;0	0;0	0;0	0;0	0;0	0;0	0;0	0;0	0;0	19;11	19	49	38.8	61.2
	CT	142	55	58	67	159	72	210	38	91	116	21	1029		
	DPA (%)	85.2	85.5	81.0	97.0	35.9	86.1	87.1	97.4	97.8	63.8	90.5			
	FPA (%)	88.0	89.1	86.2	98.5	93.7	90.3	99.5	97.4	97.8	79.3	95.2			
	DOA (%): 77.8; FOA (%): 92.4														

4. Discussion

This effort builds on the work of Foster et al. [16], Halls et al. [21], and Young et al. [19] by using machine learning algorithms to develop spatially explicit predictions of barrier island habitat based on

landscape position information. We found that the flexibility of machine learning algorithms makes them well-suited to predict barrier island habitats. In some cases, the individual parameters followed Gaussian distributions for particular habitats (Figure 6a,b); however, the distributions can become complex in the *n*-dimensional space (Figure 6c). Furthermore, machine learning algorithms are not concerned with multicollinearity from the predictor variables that could be problematic for traditional models, such as multinomial logistic regression, but instead the main concern with machine learning is how well the model can generalize to new data [50,53]. The deterministic overall accuracy for the contemporary model was just under 70%, and the fuzzy overall accuracy was just over 80%, whereas the hindcast deterministic overall accuracy was just under 80%, and the fuzzy overall accuracy was over 90%.

One challenge with the use of data-driven machine learning algorithms is that the algorithm can only learn relationships that are present in the training dataset. This can be problematic for dynamic environments, such as barrier islands, where habitat transition zones can change rapidly from the impact of an episodic event, such as a storm. The data-driven nature of machine learning algorithms underscores the need for a theoretical basis in the selection of predictor variables, as done with this study. Similarly, the results of a model can be assessed to ensure they comply with our theoretical understanding of barrier island habitats through post-processing routines similar to the ones we utilized. While the post-processing routines we used reduced the accuracies of some classes, the reduction was often associated with a minor increase in omission error. This tradeoff was justified by the overall positive increase in performance (Figure 7; Table A5) and overall comparison with habitat coverage (i.e., supratidal/upland) in the 2015 habitat map (Figure 8). In order to reduce issues associated with the data-driven approach, future efforts could aim to augment time for space by developing additional training data from historical habitat maps paired with landscape position information. Additionally, details regarding precedent conditions relating to storminess could be added to such a training dataset using an approach similar to Mickey et al. [54] to characterize storminess for a period. While we used standard presets, a more robust training dataset would allow for model preset optimization. Additionally, variables that pertain to longer-term, larger-scale variables similar to the ones used by Gutierrez et al. [14], such as island width and historical shoreline erosion rates, could also provide valuable information to improve barrier island habitat models.

In addition to utilizing post-processing to refine the models results, the use of fuzzy accuracy also helped better evaluate the performance of a model because of the flexibility to note uncertainties regarding the vegetative state of areas for a given time. For example, some areas were predicted to be intertidal marsh based on landscape position in the hindcast results, yet these areas only had sparse vegetation in the orthophotography used for validation and, at that time, may be more appropriately predicted as intertidal flat instead of intertidal marsh. In other words, an area could be predicted to be intertidal marsh based on landscape position, yet it may not be intertidal marsh at the time of assessment because it often takes time for habitat succession necessary for a marsh to develop [55]. Additionally, because of the data availability there can be a temporal lag between the acquisitions of lidar data used for model development and orthophotography used for model validation. Similarly, moving from a detailed habitat map [28] to a general model based on landscape position information required some generalizations for habitat classes. For instance, the barrier flat habitat model class (Figure 3; Table A1) includes a wide spectrum of vegetation levels, from densely vegetated meadow habitat to sparsely vegetated barrier flat [28]. The reason for this type of generalization was because of the difficulty of predicting vegetation succession from a model with landscape position alone, as the vegetation state is largely controlled by exposure to abiotic factors such as inundation and overwash from storm surges. Future research is needed to explore how landscape position and temporal lag from disturbances impact the probability of an area being vegetated.

While there are developed areas on Dauphin Island, we did not incorporate urban growth into our model. We assumed development was constant and excluded these areas from validation. Alternatively, this model framework could be used to predict potential habitat for developed areas

based on landscape position. If a researcher is interested in integrating urban growth into this type of model framework, utilizing or calibrating an existing urban growth model, such as the SLEUTH model (Slope, Land cover, Exclusion, Urbanization, Transportation, and Hillshade) similar to Terando et al. [56], may be desirable.

While our model predictor variables were developed from high-resolution lidar DEMs (i.e., 1 m to 3 m spatial resolution), we opted to use 10 m as the spatial resolution to show how a model could be applied to forecast applications, which can have variable cross-shore and alongshore resolutions [15]. We expect that using a higher resolution model grid would increase the prediction performance for the dune class based on the increased ability to resolve relative topography from higher resolution data. If we were not focused on forecasting, the model framework outlined in this effort could be calibrated with high-resolution data. Similarly, while our effort focused on developing a model to predict habitats from a DEM alone, the landscape position information used in this study could be applied to machine learning algorithms for producing contemporary or historical barrier island habitat maps with remotely sensed imagery and lidar data.

The model framework presented here can be calibrated and extended to other islands. While our effort developed a single global model for Dauphin Island, future efforts may explore the utility of developing local models based on wave energy settings and habitat composition. For instance, the orientation of an island could be used as an indicator of the need for a separate model. Dauphin Island is generally parallel to the mainland (i.e., generally east to west), whereas portions of the island run from the northwest to the southeast (Figure 2). Likewise, topographic state metrics could be used to develop meaningful model zones [18] using methods similar to that of Monge and Stallins [57].

The advantage of developing a model largely based on information that could be extracted from a TBDEM is that such a model can be calibrated and used with numerical models for forecasting alternative future states of an island with accelerated sea-level rise and simulated storms. Landscape position-based habitat models can be coupled with hydrodynamic geomorphology models [15] that incorporate coastal morphodynamics and dune evolution. Collectively, these types of models can provide natural resource managers with tools for predicting the potential future states of these ecosystems with and without management actions (e.g., beach nourishment, dune creation or restoration, and marsh creation or restoration).

5. Conclusions

Our first research question explored whether machine learning algorithms could be used to predict habitat on barrier islands based on landscape position information. We found that commonly used algorithms can predict barrier island habitats with acceptable accuracy and efficiency. The model performances among the KNN, SVM, and RF models were similar for the subtidal zone, but we opted for the KNN model based on a smoother transition from water-estuarine to water-marine. We found that RF was the best model for the intertidal and supratidal/upland zones. The deterministic overall accuracy for the contemporary model was just under 70%, and the fuzzy overall accuracy was just over 80%. For our next research question, we tested whether model performance was enhanced using post-processing routines. While this process introduced some omission error in certain classes, such as water-fresh and dune classes, the post-processing routines, collectively, tended to enhance the model results via increases in accuracy and overall comparison with habitat coverage from the source map used for training data development. For our last question, we explored how well the model would generalize to new data through a hindcast. The hindcast deterministic overall accuracy was just under 80%, and the fuzzy overall accuracy was over 90%. This model framework could be coupled with hydrodynamic geomorphology models that could incorporate coastal morphodynamics and dune evolution for forecasting alternative states of barrier islands with and without various management actions. It could also be used for producing contemporary or historical detailed barrier island habitat maps using remotely sensed imagery and lidar.

Author Contributions: N.M.E., L.W., H.W. conceived and designed the study; N.M.E., M.J.O., L.C.F., S.M.B., and R.H.D. collected the data; N.M.E. and L.W. analyzed the data; N.M.E. wrote the paper; all authors contributed critically to subsequent drafts and gave final approval for publication.

Funding: This effort supported one component of a larger collaborative effort between the U.S. Army Corps of Engineers, the State of Alabama, and the U.S. Geological Survey, funded by the National Fish and Wildlife Foundation Gulf Environmental Benefit Fund (project ID: 45719) to investigate viable, sustainable restoration options that protect and restore the natural resources of Dauphin Island, Alabama.

Acknowledgments: We thank Yi Qiang (University of Hawai'i) and Nina Lam (Louisiana State University) for providing an introduction to using MATLAB for machine learning classification applications. We thank Stephen DeMaso from the U.S. Fish and Wildlife Service and three anonymous reviewers for reviewing this work. Any use of trade, firm, or product names is for descriptive purposes only and does not imply endorsement by the U.S. Government. This manuscript is submitted for publication with the understanding that the U.S. Government is authorized to reproduce and distribute reprints for Governmental purposes. Data developed for this study are publicly archived at https://doi.org/10.5066/P90MACYS.

Conflicts of Interest: The authors declare no conflict of interest.

Appendix A

Table A1. Descriptions of the habitat classes included in the habitat model for Dauphin Island, Alabama, USA.

Habitat	Description	Source
Barrier flat	Barrier flat includes flat or gently sloping supratidal/upland areas that are located on the backslope of dunes, unvegetated washover fans, and areas along estuarine shorelines. Barrier flat habitat can be unvegetated or vegetated (i.e., meadow).	[9,35]
Beach	Beach includes bare or sparsely vegetated supratidal areas that are located upslope of the intertidal beach and marine-water habitats. These habitats are located along shorelines with high wave energy.	[44]
Developed [1]	Developed includes areas dominated by constructed materials (i.e., transportation infrastructure, residential, and commercial areas).	[58]
Dune	Dunes are supratidal features developed via Aeolian processes with a well-defined relative elevation. Dune habitat can be vegetated or unvegetated.	[59]
Intertidal beach	Intertidal beach includes bare or sparsely vegetated intertidal wetlands located along the ocean-facing side of the island that are adjacent to high-energy shorelines.	[44]
Intertidal flat	Intertidal flat includes bare or sparsely vegetated intertidal wetlands that are adjacent to estuarine-water and along low-energy shorelines.	[44]
Intertidal marsh	Intertidal marsh includes all intertidal wetlands with 30 percent or greater areal cover by erect, rooted, herbaceous hydrophytes.	[44]
Water-estuarine	Water-estuarine includes all areas of subtidal water and ponds on the back-barrier side of the island. These areas rarely have salinity greater than 30 parts per thousand and generally have less than 30 percent cover of vegetation.	[44]
Water-fresh	Water-fresh includes all areas of supratidal/upland water that generally have less than 30 percent cover of vegetation.	[44]
Water-marine	Water-marine includes all areas of subtidal water found offshore of the ocean-facing side of the island. These areas are found along high-energy coastlines and/or are areas that occasionally experience salinity levels greater than or equal to 30 parts per thousand and generally have less than 30 percent cover of vegetation.	[44]
Woody vegetation	Woody vegetation includes supratidal/upland scrub/shrub and forested areas where woody vegetation height is greater than about 0.5 m. Woody vegetation coverage should generally be greater than 30 percent.	[44,58]
Woody wetland	Woody wetland includes all supratidal/upland wetlands dominated by woody vegetation with a vegetation height greater than about 0.5 m. Woody vegetation coverage should generally be greater than 30 percent.	[44]

[1] Developed was not modeled in this effort. We assumed there were no changes in developed areas from the 2015 habitat map.

Table A2. Model presets and overall accuracy results using five-fold cross validation by algorithm (i.e., K-nearest neighbor, support vector machine, and random forest models) for the subtidal zone for the contemporary habitat model development for Dauphin Island, Alabama, USA. D: Distance; K = Number of neighbors; KT: Kernel type; KS: Kernel scale; SD: Standard deviation; and W: Weight.

Algorithm	Name	Configuration	Overall Accuracy	
			Mean	SD
K-nearest neighbor (KNN)	Fine KNN	K = 1; D = Euclidean	94.60	0.15
	Medium KNN	K = 10; D = Euclidean	96.16	0.16
	Coarse KNN	K = 100; D = Euclidean	96.54	0.05
	Cosine KNN	K = 10; D = cosine	96.20	0.14
	Cubic KNN	K = 10; D = cubic	96.16	0.16
	Weighted KNN	K = 10; D = Euclidean; W = inverse squared	94.82	0.10
Support vector machine (SVM)	Linear SVM	KT = linear; KS = automatic	96.48	0.04
	Quadratic SVM	KT = quadratic; KS = automatic	96.50	0.00
	Cubic SVM	KT = cubic; KS = automatic	92.62	4.50
	Fine Gaussian SVM	KT = Gaussian; KS = 0.56	96.52	0.04
	Medium Gaussian SVM	KT = Gaussian; KS = 2.2	96.50	0.06
	Coarse Gaussian SVM	KT = Gaussian; KS = 8.9	93.30	0.00
Random forest (RF)	Random forest	30 trees	94.64	0.20

Table A3. Model presets and overall accuracy results using five-fold cross validation by algorithm (i.e., K-nearest neighbor, support vector machine, and random forest models) for the intertidal zone for the contemporary habitat model development for Dauphin Island, Alabama, USA. D: Distance; K = Number of neighbors; KT: Kernel type; KS: Kernel scale; SD: Standard deviation; and W: Weight.

Algorithm	Name	Configuration	Overall Accuracy	
			Mean	SD
K-nearest neighbor (KNN)	Fine KNN	K = 1; D = Euclidean	82.54	0.82
	Medium KNN	K = 10; D = Euclidean	82.46	1.15
	Coarse KNN	K = 100; D = Euclidean	72.66	0.23
	Cosine KNN	K = 10; D = cosine	81.22	0.84
	Cubic KNN	K = 10; D = cubic	81.22	1.65
	Weighted KNN	K = 10; D = Euclidean; W = inverse squared	84.68	1.63
Support vector machine (SVM)	Linear SVM	KT = linear; KS = automatic	80.74	0.53
	Quadratic SVM	KT = quadratic; KS = automatic	84.22	0.48
	Cubic SVM	KT = cubic; KS = automatic	85.54	1.00
	Fine Gaussian SVM	KT = Gaussian; KS = 0.56	84.34	0.55
	Medium Gaussian SVM	KT = Gaussian; KS = 2.2	81.60	0.60
	Coarse Gaussian SVM	KT = Gaussian; KS = 8.9	71.58	0.48
Random forest (RF)	Random forest	30 trees	88.78	0.63

Table A4. Model presets and overall accuracy results using five-fold cross validation by algorithm (i.e., K-nearest neighbor, support vector machine, and random forest models) for the supratidal/upland zone for the contemporary habitat model development for Dauphin Island, Alabama, USA. D: Distance; K = Number of neighbors; KT: Kernel type; KS: Kernel scale; SD: Standard deviation; and W: Weight.

Algorithm	Name	Configuration	Overall Accuracy	
			Mean	SD
K-nearest neighbor (KNN)	Fine KNN	K = 1; D = Euclidean	71.26	0.35
	Medium KNN	K = 10; D = Euclidean	74.02	0.51
	Coarse KNN	K = 100; D = Euclidean	66.22	0.19
	Cosine KNN	K = 10; D = cosine	72.64	0.42
	Cubic KNN	K = 10; D = cubic	73.56	0.67
	Weighted KNN	K = 10; D = Euclidean; W = inverse squared	75.74	0.87
Support vector machine (SVM)	Linear SVM	KT = linear; KS = automatic	72.74	0.22
	Quadratic SVM	KT = quadratic; KS = automatic	76.36	0.34
	Cubic SVM	KT = cubic; KS = automatic	75.62	0.65
	Fine Gaussian SVM	KT = Gaussian; KS = 0.56	70.74	0.52
	Medium Gaussian SVM	KT = Gaussian; KS = 2.2	74.08	0.43
	Coarse Gaussian SVM	KT = Gaussian; KS = 8.9	64.62	0.12
Random forest (RF)	Random forest	30 trees	78.02	0.64

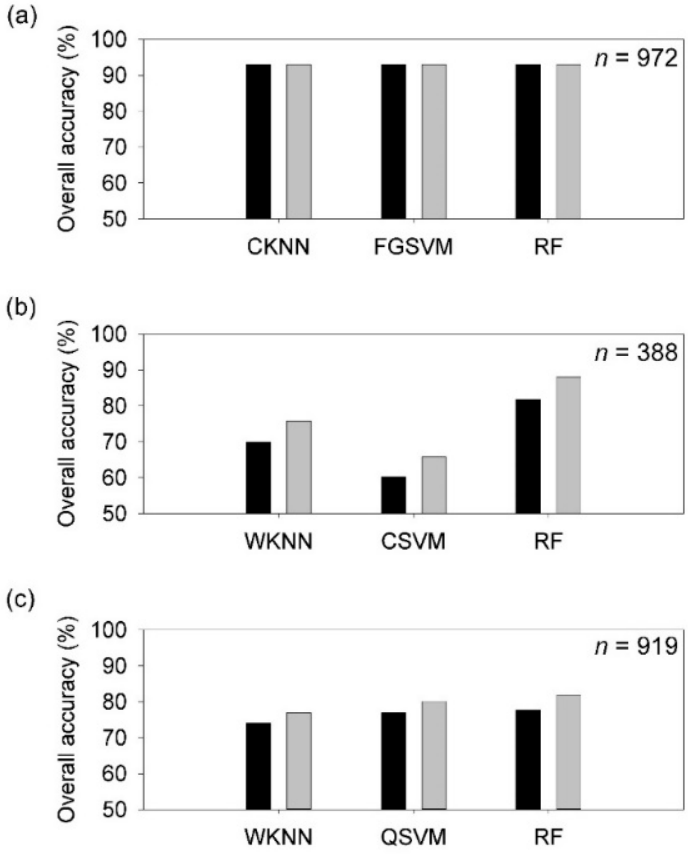

Figure A1. Deterministic accuracy (black bar) and fuzzy overall accuracy (gray bar) by zone for the top three models for the contemporary habitat model development for Dauphin Island, Alabama, USA. (**a**) Subtidal zone; (**b**) Intertidal zone; and (**c**) Supratidal/upland zone. CKNN: Coarse K-nearest neighbor model; CSVM: Cubic support vector machine model; FGSVM: Fine-scaled Gaussian support vector machine model; RF: Random forest model; QSVM: Quadratic support vector machine model; and WKNN: Weighted K-nearest neighbor model.

Table A5. McNemar's test results (*p*-values) for determining whether there is a significant difference between model performance for (**a**) top-performing intertidal zone models; (**b**) top-performing supratidal zone models; and (**c**) contemporary model with various levels of post-processing. CSVM: Cubic support vector machine model; NPP: Combined model with no post-processing; RF: Random forest model; QSVM: Quadratic support vector machine model; WKNN: Weighted K-nearest neighbor model; WPP: Combined model with post-processing, but no minimum mapping unit; WPP+MMU: Combined model with post-processing and minimum mapping unit; *: Significant at the $p < 0.05$ level; and **: Significant at the $p < 0.001$ level.

(a)		**Deterministic**		**Fuzzy**	
		WKNN	CSVM	WKNN	CSVM
	RF	**	**	**	**
	WKNN	NA	**	NA	**
(b)		**Deterministic**		**Fuzzy**	
		RF	QSVM	RF	QSVM
	RF	*	0.617	**	0.126
	WKNN	NA	*	NA	*
(c)		**Deterministic**		**Fuzzy**	
		WPP	WPP+MMU	WPP	WPP+MMU
	NPP	0.267	0.108	**	**
	WPP	NA	0.230	NA	0.264

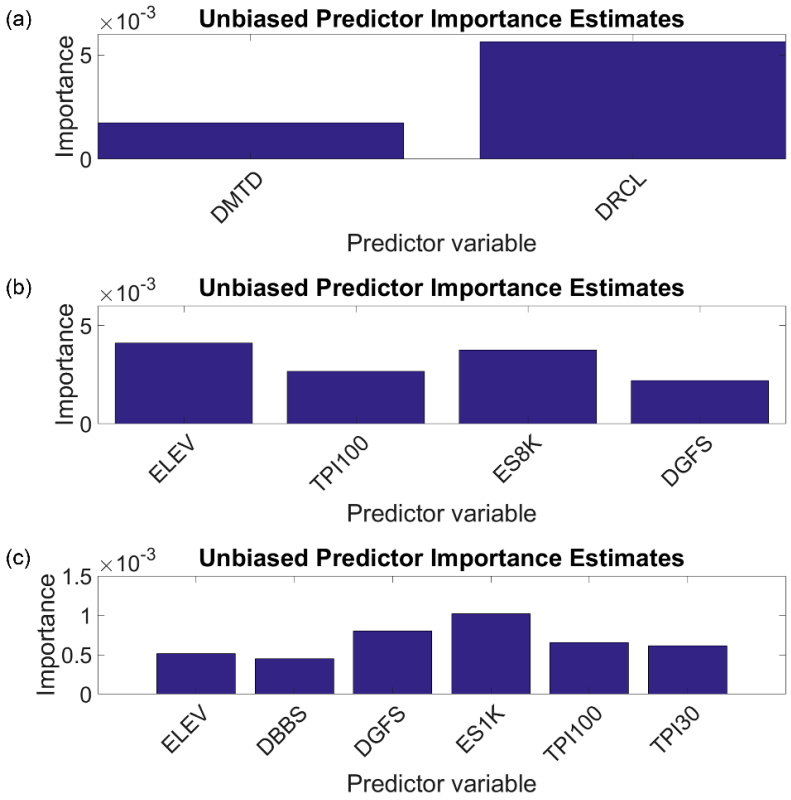

Figure A2. Unbiased predictor importance estimates by model zone for the contemporary habitat model fitting Dauphin Island, Alabama, USA. (**a**) Subtidal zone; (**b**) intertidal zone; and (**c**) supratidal/upland zone. DBBS: Distance from back-barrier shoreline; DGFS: Distance from ocean-facing shoreline; DMTD: Distance from Mobile-Tensaw River Delta; DRCL: Direction from center; Elevation; ELEV: Elevation; ES1K: Elevation to the south (1 km); ES8K: Elevation to the south (8 km); TPI30: Topographic position index (30 m); TPI100: Topographic position index (100 m).

Table A6. The type, condition, and order for user-defined rules applied to model results via post-processing by habitat class for the habitat model for Dauphin Island, Alabama, USA.

Type of Correction	Habitat	Condition	Order
Elevation	Dune	Dune areas that had a probability less than 0.5 for being above the extreme storm water level were changed to barrier flat.	2
Elevation - depressional habitats	Barrier flat	Barrier flat areas that had a sink depth greater than or equal to 0.5 m were changed to water-fresh.	11
	Intertidal beach	Intertidal beach areas that had a sink depth greater than or equal to 0.01 m should be commonly inundated with standing water and were changed to water-marine.	7
	Intertidal flat	Intertidal flat areas that had a sink depth greater than or equal to 0.01 m should be commonly inundated with standing water and were changed to water-estuarine.	8
	Water-fresh	Water-fresh areas that did not have a sink depth greater than or equal to 0.5 m were changed to barrier flat.	10
	Woody wetland	Woody wetland areas that did not have a sink depth greater than or equal to 0.1 m were recoded to be woody vegetation.	1

Table A6. *Cont.*

Type of Correction	Habitat	Condition	Order
X,Y coordinates	Intertidal beach	Intertidal beach areas that were found to be closer to the back-barrier shoreline than the ocean-facing shoreline were changed to intertidal flat.	3
	Barrier flat	Barrier flat areas that had intertidal beach within a 5-by-5 pixel neighborhood were changed to beach due to the proximity to the ocean-facing shoreline.	9
	Intertidal beach	Intertidal beach areas that were located behind supratidal areas with an elevation to the south for 1 km greater than or equal to 0.6 m were changed to intertidal flat.	5
	Intertidal flat	Intertidal flat areas that were closer to water-marine than water-estuarine were changed to intertidal flat.	6
	Intertidal marsh/ Intertidal flat	Intertidal marsh areas should be sheltered from high-energy areas (Roland & Douglass, 2005). These areas that did not have an elevation to the south for 8 km greater than or equal to 0.448 m (i.e., EHWS) were changed to intertidal beach. This rule was also applied to intertidal flat.	4

Table A7. Error matrix with deterministic and fuzzy accuracies for the initial contemporary model results (i.e., without post-processing and a four-pixel minimum mapping unit) for Dauphin Island, Alabama, USA. For the off-diagonal cells, the first value indicates deterministic count and the second value indicates the fuzzy count. BF: Barrier flat; B: Beach; CT: Column total; D: Dune; DPA: Deterministic producer's accuracy; DOA: Deterministic overall accuracy; DUA: Deterministic user's accuracy; FOA: Fuzzy overall accuracy; FPA: Fuzzy producer's accuracy; FUA: Fuzzy user's accuracy; IB: Intertidal beach; IF: Intertidal flat; IM: Intertidal marsh; RT: Row total; WE: Water-estuarine; WF: Water-fresh; WM: Water-marine; WV: Woody vegetation; and WW: Woody wetland.

	Class	Reference Data											RT	DUA (%)	FUA (%)
		BF	B	D	IB	IF	IM	WE	WF	WM	WV	WW			
Model data	BF	305	4;2	36;1	1;0	15;8	47;23	13;0	0;0	0;0	31;15	0;0	501	60.9	70.7
	B	4;7	62	0;1	2;14	0;3	3;0	1;0	0;0	7;25	0;1	0;0	130	47.7	86.9
	D	38;1	0;1	99	0;0	0;0	0;0	0;0	0;0	3;1	5;1	0;0	149	66.4	69.1
	IB	1;0	13;1	0;0	17	0;2	1;0	0;10	0;0	2;88	0;0	0;0	135	12.6	87.4
	IF	17;5	4;0	0;0	3;0	95	39;34	73;144	0;0	11;0	2;1	0;0	428	22.2	65.2
	IM	13;6	2;0	2;0	0;0	23;4	307	54;3	0;0	1;0	1;1	0;0	417	73.6	77.0
	WE	1;0	0;0	0;0	0;0	0;0	0;0	607	0;0	0;0	0;0	0;0	608	99.8	99.8
	WF	9;0	0;0	0;0	0;0	0;0	0;0	9;0	27	1;0	4;1	0;0	51	52.9	54.9
	WM	0;0	1;0	0;0	0;0	0;0	0;0	68;0	0;0	314	0;0	0;0	383	82.0	82.0
	WV	13;8	0;0	0;0	0;0	0;0	6;0	0;0	0;0	0;0	205	2;0	234	87.6	91.0
	WW	2;0	0;0	0;0	0;0	0;0	0;0	0;0	1;0	0;0	20;3	29	55	52.7	58.2
	CT	430	90	139	37	150	460	982	28	453	291	31	3091		
	DPA (%)	70.9	68.9	71.2	46.0	63.3	66.7	61.8	96.4	69.3	70.5	93.6			
	FPA (%)	77.2	73.3	72.7	83.8	74.7	79.1	77.8	96.4	94.5	78.4	93.6			
		DOA (%): 66.9; FOA (%): 80.3													

References

1. Oertel, G.F. The Barrier Island System. *Mar. Geol.* **1985**, *63*, 1–18. [CrossRef]
2. Stutz, M.L.; Pilkey, O.H. Open-Ocean Barrier Islands: Global Influence of Climatic, Oceanographic, and Depositional Settings. *J. Coast. Res.* **2011**, *27*, 207–222. [CrossRef]
3. Barbier, E.B.; Hacker, S.D.; Kennedy, C.; Koch, E.W.; Stier, A.C.; Silliman, B.R. The value of estuarine and coastal ecosystem services. *Ecol. Monogr.* **2011**, *81*, 169–193. [CrossRef]
4. Feagin, R.A.; Smith, W.K.; Psuty, N.P.; Young, D.R.; Martínez, L.M.; Carter, G.A.; Lucas, K.L.; Gibeaut, J.C.; Gemma, J.N.; Koske, R.E. Barrier Islands: Coupling Anthropogenic Stability with Ecological Sustainability. *J. Coast. Res.* **2010**, *26*, 987–992. [CrossRef]
5. Sallenger, A.H. Storm impact scale for barrier islands. *J. Coast. Res.* **2000**, *16*, 890–895.
6. Campbell, A.; Wang, Y.; Christiano, M.; Stevens, S. Salt Marsh Monitoring in Jamaica Bay, New York from 2003 to 2013: A Decade of Change from Restoration to Hurricane Sandy. *Remote Sens.* **2017**, *9*, 131. [CrossRef]

7. Jeter, G.W., Jr.; Carter, G.A. Habitat change on Horn Island, Mississippi, 1940–2010, determined from textural features in panchromatic vertical aerial imagery. *Geocarto Int.* **2015**, *31*, 985–994. [CrossRef]
8. Kindinger, J.L.; Buster, N.A.; Flocks, J.G.; Bernier, J.C.; Kulp, M.A. *Louisiana Barrier Island Comprehensive Monitoring (BICM) Program Summary Report: Data and Analyses 2006 through 2010*; U.S. Geological Survey: Reston, VA, USA, 2013; p. 86.
9. Lucas, K.L.; Carter, G.A. Decadal Changes in Habitat-Type Coverage on Horn Island, Mississippi, U.S.A. *J. Coast. Res.* **2010**, *26*, 1142–1148. [CrossRef]
10. Zinnert, J.C.; Shiflett, S.A.; Via, S.; Bissett, S.; Dows, B.; Manley, P.; Young, D.R. Spatial–Temporal Dynamics in Barrier Island Upland Vegetation: The Overlooked Coastal Landscape. *Ecosystems* **2016**, *19*, 685–697. [CrossRef]
11. Pilkey, O.H.; Cooper, J.A.G. *The Last Beach*; Duke University Press: Durham, UK; London, UK, 2014.
12. Hansen, J.; Sato, M.; Hearty, P.; Ruedy, R.; Kelley, M.; Masson-Delmotte, V.; Russell, G.; Tselioudis, G.; Cao, J.; Rignot, E.; et al. Ice melt, sea level rise and superstorms: Evidence from paleoclimate data, climate modeling, and modern observations that 2 °C global warming could be dangerous. *Atmos. Chem. Phys.* **2016**, *16*, 3761–3812. [CrossRef]
13. Knutson, T.R.; McBride, J.L.; Chan, J.; Emanuel, K.; Holland, G.; Landsea, C.; Held, I.; Kossin, J.P.; Srivastava, A.K.; Sugi, M. Tropical cyclones and climate change. *Nat. Geosci.* **2010**, *3*, 157–163. [CrossRef]
14. Guiterrez, B.T.; Plant, N.G.; Thieler, E.R.; Turecek, A. Using a Bayesian network to predict barrier island geomorphologic characteristics. *J. Geophys. Res. Earth Surf.* **2015**, *120*, 2452–2475. [CrossRef]
15. Passeri, D.L.; Long, J.W.; Plant, N.G.; Bilskie, M.V.; Hagen, S.C. The influence of bed friction variability due to land cover on storm-driven barrier island morphodynamics. *Coast. Eng.* **2018**, *132*, 82–94. [CrossRef]
16. Foster, T.E.; Stolen, E.D.; Hall, C.R.; Schaub, R.; Duncan, B.W.; Hunt, D.K.; Drese, J.H. Modeling vegetation community responses to sea-level rise on Barrier Island systems: A case study on the Cape Canaveral Barrier Island complex, Florida, USA. *PLoS ONE* **2017**, *12*, e0182605. [CrossRef] [PubMed]
17. Dayton, P.K. Toward an understanding of community resilience and the potential effects of enrichments to the benthos at McMurdo Sound, Antarctica. In Proceedings of the Colloquium on Conservation Problems in Antarctica, Blacksburg, VA, USA, 10–12 September 1971; Parker, B.C., Ed.; Allen Press: Lawrence, KS, USA, 1972; pp. 81–96.
18. Zinnert, J.C.; Stallins, J.A.; Brantley, S.T.; Young, D.R. Crossing Scales: The Complexity of Barrier-Island Processes for Predicting Future Change. *BioScience* **2017**, *67*, 39–52. [CrossRef]
19. Young, D.R.; Brantley, S.T.; Zinnert, J.C.; Vick, J.K. Landscape position and habitat polygons in a dynamic coastal environment. *Ecosphere* **2011**, *2*, 1–15. [CrossRef]
20. Anderson, C.P.; Carter, G.A.; Funderburk, W.A. The Use of Aerial RGB Imagery and LIDAR in Comparing Ecological Habitats and Geomorphic Features on a Natural versus Man-Made Barrier Island. *Remote Sens.* **2016**, *8*, 602. [CrossRef]
21. Halls, J.N.; Frishman, M.A.; Hawkes, S.C. An Automated Model to Classify Barrier Island Geomorphology Using Lidar Data and Change Analysis (1998–2014). *Remote Sens.* **2018**, *11*, 1109. [CrossRef]
22. Barandela, R.; Juarez, M. Supervised classification of remotely sensed data with ongoing learning capability. *Int. J. Remote Sens.* **2002**, *23*, 4965–4970. [CrossRef]
23. Manton, M.G.; Angelstam, P.; Mikusiński, G. Modelling habitat suitability for deciduous forest focal species—A sensitivity analysis using different satellite land cover data. *Landsc. Ecol.* **2005**, *20*, 827–839. [CrossRef]
24. Guo, Q.; Kelly, M.; Graham, C.H. Support vector machines for predicting distribution of Sudden Oak Death in California. *Ecol. Model.* **2005**, *182*, 75–90. [CrossRef]
25. Heumann, B.W. An Object-Based Classification of Mangroves Using a Hybrid Decision Tree—Support Vector Machine Approach. *Remote Sens.* **2011**, *3*, 2440–2460. [CrossRef]
26. Prasad, A.M.; Iverson, L.R.; Liaw, A. Newer classification and regression tree techniques: Bagging and random forests for ecological prediction. *Ecosystems* **2006**, *9*, 181–199. [CrossRef]
27. Rogan, J.; Franklin, J.; Roberts, D.A. A comparison of methods for monitoring multitemporal vegetation change using Thematic Mapper imagery. *Remote Sens. Environ.* **2002**, *80*, 143–156. [CrossRef]
28. Enwright, N.M.; Wang, L.; Borchert, S.M.; Day, R.H.; Feher, L.C.; Osland, M.J. Advancing barrier island habitat mapping using landscape position information and elevation uncertainty. *Prog. Phys. Geogr.* **2019**. [CrossRef]

29. McCarthy, M.J.; Halls, J.N. Habitat Mapping and Change Assessment of Coastal Environments: An Examination of WorldView-2, QuickBird, and IKONOS Satellite Imagery and Airborne LiDAR for Mapping Barrier Island Habitats. *ISPRS Int. J. Geo-Inf.* **2014**, *3*, 297–325. [CrossRef]
30. Buffington, K.J.; Dugger, B.D.; Thorne, K.M.; Takekawa, J.Y. Statistical correction of lidar-derived digital elevation models with multispectral airborne imagery in tidal marshes. *Remote Sens. Environ.* **2016**, *186*, 616–625. [CrossRef]
31. Medeiros, S.; Hagen, S.; Weishampel, J.; Angelo, J. Adjusting Lidar-Derived Digital Terrain Models in Coastal Marshes Based on Estimated Aboveground Biomass Density. *Remote Sens.* **2015**, *7*, 3507–3525. [CrossRef]
32. Enwright, N.M.; Wang, L.; Borchert, S.M.; Day, R.H.; Feher, L.C.; Osland, M.J. The impact of lidar elevation uncertainty on mapping intertidal habitats on barrier islands. *Remote Sens.* **2018**, *10*, 5. [CrossRef]
33. Wernette, P.; Houser, C.; Bishop, M.P. An automated approach for extracting Barrier Island morphology from digital elevation models. *Geomorphology* **2016**, *262*, 1–7. [CrossRef]
34. Roland, R.M.; Douglass, S.L. Estimating Wave Tolerance of Spartina alterniflora in Coastal Alabama. *J. Coast. Res.* **2005**, *21*, 453–463. [CrossRef]
35. Leatherman, S.P. *Barrier Island Handbook*; National Park Service: Amherst, MA, USA, 1979.
36. Mcbride, R.A.; Anderson, J.B.; Buynevich, I.V.; Cleary, W.; Fenster, M.S.; FitzGerald, D.M.; Harris, M.S.; Hein, C.J.; Klein, A.H.F.; Liu, B.; et al. Morphodynamics of Barrier Systems: A Synthesis. In *Treatise on Geomorphology*; Coastal Geomorphology; Sherman, D.J., Ed.; Academic Press: San Diego, CA, USA, 2013; pp. 166–244.
37. Otvos, E.G.J.; Carter, G.A. Hurricane Degradation—Barrier Development Cycles, Northeastern Gulf of Mexico: Landform Evolution and Island Chain History. *J. Coast. Res.* **2008**, *24*, 463–478. [CrossRef]
38. Henderson, R.E.; Nelson, P.R.; Long, J.W.; Smith, C.G. *Vector Shorelines and Associated Shoreline Change Rates Derived from Lidar and Aerial Imagery for Dauphin Island, Alabama: 1940–2015*; U.S. Geological Survey: Reston, VA, USA, 2017.
39. DeWitt, N.T.; Stalk, C.A.; Flocks, J.G.; Bernier, J.C.; Kelso, K.W.; Fredricks, J.J.; Tuten, T. *Single-Beam Bathymetry Data Collected in 2015 Nearshore Dauphin Island, Alabama*; U.S. Geological Survey: Reston, VA, USA, 2015.
40. Thatcher, C.A.; Brock, J.C.; Danielson, J.J.; Poppenga, S.K.; Gesch, D.B.; Palaseanu-Lovejoy, M.E.; Barras, J.A.; Evans, G.A.; Gibbs, A.E. Creating a coastal national elevation database (CoNED) for science and conservation applications. *J. Coast. Res.* **2016**, *76*, 64–74. [CrossRef]
41. Bonisteel, J.M.; Nayegandhi, A.; Wright, C.W.; Brock, J.C.; Nagle, D.B. *Experimental Advanced Airborne Research Lidar (EAARL) Data Processing Manual*; U.S. Geological Survey: Reston, VA, USA, 2009; p. 38.
42. Enwright, N.M.; Borchert, S.B.; Day, R.H.; Feher, L.C.; Osland, M.J.; Wang, L.; Wang, H. *Barrier Island Habitat Map and Vegetation Survey—Dauphin Island, Alabama, 2015*; U.S. Geological Survey: Reston, VA, USA, 2017; p. 17.
43. Byrnes, M.R.; Baker, J.L.; Li, F. *Quantifying Potential Measurement Errors and Uncertainties Associated with Bathymetric Change Analysis*; U.S. Army Engineer Research and Development Center: Vicksburg, MS, USA, 2002.
44. Cowardin, L.M.; Carter, V.; Golet, F.C.; LaRoe, E.T. *Classification of Wetlands and Deepwater Habitats of the United States*; United States Department of Interior, Fish and Wildlife Service: Washington, DC, USA, 1979; p. 134.
45. Zervas, C. *Extreme Water Levels of the United States 1893–2010*; National Oceanic and Atmospheric Administration: Silver Spring, MD, USA, 2013; p. 200.
46. NOAA. Extreme Water Levels 8735180 Dauphin Island, AL Webpage. Available online: https://tidesandcurrents.noaa.gov/est/est_station.shtml?stnid=8735180 (accessed on 10 October 2018).
47. Poulter, B.; Halpin, P.N. Raster modelling of coastal flooding from sea-level rise. *Int. J. Geogr. Inf. Sci.* **2008**, *22*, 167–182. [CrossRef]
48. Weiss, A.D. Topographic Position and Landforms Analysis. *Poster Presentation, ESRI User Conference, San Diego, CA*; San Diego, CA, USA. 2001. Available online: http://www.jennessent.com/downloads/TPI-poster-TNC_18x22.pdf (accessed on 30 October 2018).
49. Congalton, R.G.; Green, K. *Assessing the Accuracy of Remotely Sensed Data Principles and Practices*; CRC Press: Boca Raton, FL, USA, 2009.
50. James, G.; Witten, D.; Hastie, T.; Tibshirani, R. *An Introduction to Statistical Learning: With Applications in R*; Springer New York: New York, NY, USA, 2013.

51. Woodcock, C.E.; Gopal, S. Fuzzy set theory and thematic maps: Accuracy assessment and area estimation. *Int. J. Geogr. Inf. Sci.* **2000**, *14*, 153–172. [CrossRef]
52. Foody, G.M. Thematic Map Comparison: Evaluating the Statistical Significance of Differences in Classification Accuracy. *Photogramm. Eng. Remote Sens.* **2004**, *70*, 627–633. [CrossRef]
53. Shumeli, G. To Explain or to Predict? *Stat. Sci.* **2010**, *25*, 289–310. [CrossRef]
54. Mickey, R.C.; Long, J.W.; Plant, N.G.; Thompson, D.M.; Dalyander, P.S. *A Methodology for Modeling Barrier Island Storm-Impact Scenarios*; U.S. Geological Survey: Reston, VA, USA, 2017; p. 17.
55. Mitsch, W.J.; Wilson, R.F. Improving the Success of Wetland Creation and Restoration with Know-How, Time, and Self-Design. *Ecol. Appl.* **1996**, *6*, 77–83. [CrossRef]
56. Terando, A.J.; Costanza, J.; Belyea, C.; Dunn, R.R.; McKerrow, A.; Collazo, J.A. The southern megalopolis: Using the past to predict the future of urban sprawl in the southeast U.S. *PLoS ONE* **2014**, *9*, e102261. [CrossRef]
57. Monge, J.A.; Stallins, J.A. Properties of dune topographic state space for six barrier islands of the U.S. Southeastern Atlantic Coast. *Phys. Geogr.* **2016**, *37*, 452–475. [CrossRef]
58. Homer, C.G.; Dewitz, J.A.; Yang, L.; Jin, S.; Danielson, P.; Xian, G.; Coulston, J.; Herold, N.D.; Wickham, J.D.; Megown, K. Completion of the 2011 National Land Cover Database for the conterminous United States-Representing a decade of land cover change information. *Photogramm. Eng. Remote Sens.* **2015**, *81*, 345–354. [CrossRef]
59. Acosta, A.; Carranza, M.L.; Izzi, C.F. Combining land cover mapping of coastal dunes with vegetation analysis. *Appl. Veg. Sci.* **2005**, *8*, 133–138. [CrossRef]